International Journal of Thermophysics, Vol. 9, No. 4, 1988

The Influence of Residual Gas Pressure on the Thermal Conductivity of Microsphere Insulations

R. Wawryk[1] **and J. Rafalowicz**[1]

Received April 1, 1988

Experimental results of investigations of the heat exchange by residual gas in microsphere insulations are presented. The results of measurements of microsphere effective thermal conductivity versus residual gas (N_2) pressure in the pressure range of 10^{-3}–10^5 Pa are also given. A sample of self-pumping microsphere insulation was prepared and its thermal parameters were tested. In comparison to the standard microsphere insulation, the self-pumping insulation yielded lower thermal conductivity results over the entire pressure range. The stability of its thermal parameters as a result of considerable gas input into the insulation volume is discussed. Measurements of temperature and pressure distributions inside the microsphere layer were performed. Plots of temperature and pressure gradients inside the layer of the microsphere insulation are presented.

KEY WORDS: heat transfer; insulation; microspheres, thermal conductivity.

1. INTRODUCTION

Residual gas is an important heat transfer medium in microsphere insulation. It was found that the simultaneous evacuation of the insulation and heating lowers the gas pressure not only in the void space between spheres but also inside the microspheres. The latter is related to gas diffusion via the microsphere walls. Another source of the residual gas is the desorption of gas molecules from the microsphere material. In order to decrease the contribution of gas to the total heat transfer in microsphere insulation as it is done in the multilayer insulation [1], Wawryk and Balcerek [2] applied a sorbent which decreases the gas pressure in the interstitial volume. The mixture of microspheres with powdered sorbent

[1] Institute for Low Temperature and Structure Research, Polish Academy of Sciences, 95 Prochnik Street, 53 529 Wroclaw, Poland.

0195-928X/88/0700-0611$06.00/0

with a diameter of the order of 1 μm is referred to as the self-pumping microsphere insulation.

Heat transfer in the microsphere insulation consists of the three important heat exchange mechanisms: (1) heat conduction by the solid state, (2) heat conduction by the residual gas, and (3) heat transfer by radiation. The effective thermal conductivity coefficient $k(T)$ may be expressed as the sum of the corresponding components:[2]

$$k(T, p) = k_c(T, p) + k_r(T) = k_{ss}(T, p) + k_{gc}(T, p) + k_r(T) \tag{1}$$

where k_c is the component of the heat transfer by conduction, k_r is the component of the heat transfer by radiation, k_{gc} is the component of the heat conduction by gas, and k_{ss} is the component of the heat conduction by the solid state. The conduction and the radiation components are discussed in Refs. 3 and 4.

The component of heat conduction by gas in a granular porous material is given by the following equation [5]:

$$k_{gc}(T, p) = k_g \left\{ \frac{5.8(1-m)^2}{K} \left[\frac{1}{K} \ln \frac{k_{gr}}{kg} - 1 - \frac{K}{2} \right] + 1 \right\} \tag{2}$$

where

$$K = 1 - \frac{kg}{k_{gr}}; \qquad k_{gr} \approx 2k_s \frac{1-m'}{2+m'}$$

and the thermal conductivity of a gas k_g may be expressed by [6]

$$k_g = k_{go} \left(1 + \frac{19}{6} \frac{2-\alpha}{\alpha} Kn \right)^{-1} \tag{3}$$

where

$$Kn = \frac{\bar{L}}{\delta_a}; \qquad \delta_a = \frac{2}{3} \frac{m}{1-m} d_m$$

The mean free path of gas molecules is expressed by [5]

$$\bar{L} = \frac{\kappa}{\bar{p}} \frac{1}{1 + (T_y/T)} \tag{4}$$

where κ and T_v are constants depending on the gas, and

$$\bar{p} = \frac{p_g(T_H^{1/2} + T_C^{1/2})}{2T_g^{1/2}}$$

For air, $\kappa = 8.42 \times 10^{-3}$ N · m^{-1}, and $T_y = 113$ K.

[2] A complete explanation of symbols is given under Nomenclature at the end of the paper.

2. RESULTS

2.1. The Influence of Residual Gas Pressure on the Thermal Conductivity

Measurements of the effective thermal conductivity coefficient as a function of the residual gas pressure $k(p)$ were performed in a calorimeter of spherical symmetry which is described in detail in Ref. 4. The use of spherical symmetry for powder-vacuum insulation is especially valuable because of elimination of boundary effects. Such kinds of calorimeters were used earlier [7, 8]. The thickness of the insulating space of the calorimeter was 2.95 cm. During an experiment, the outside wall of the calorimeter was immersed in liquid nitrogen.

Pure nitrogen was used as the residual gas. The microsphere sample had a mean diameter (d_m) of 95 μm and a density (γ) of 390 kg · m^{-3}. The composition of the shell of the microspheres was as follows: SiO_2, 56%; Al, 15%; K, 2.9%; Fe, 2%; and Na, 0.6%.

A comparison of our results with the data of Cunnington and Tien [9] is presented in Fig. 1. It may be seen that there is a qualitative agreement between the two curves for the effective thermal conductivity versus the residual gas pressure. Within the pressure range 10^{-3} to 1 Pa,

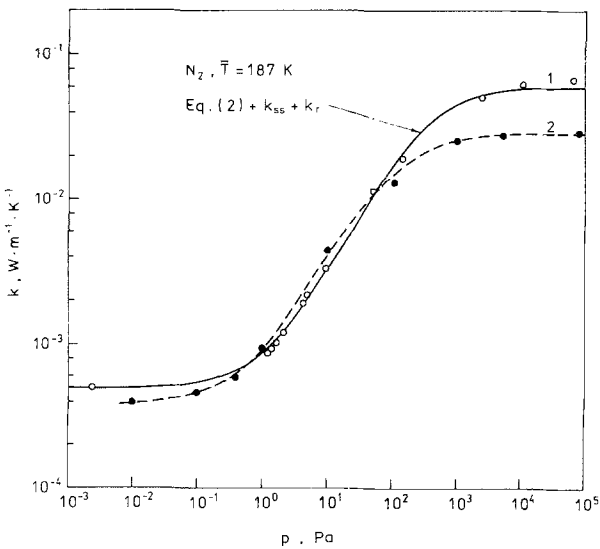

Fig. 1. Apparent thermal conductivity of microsphere insulation vs residual gas pressure (N_2). Curve 1, our results for $\bar{T} = 187$ K; line represents Eq. (2) $+ k_{ss} + k_r$, $k_{ss} + k_r = 5.03 \times 10^{-4}$ W · m^{-1} · K^{-1}. Curve 2, the data of Cunnington and Tien [9] for $\bar{T} = 200$ K.

where the conductivity by gas is negligible compared to the total insulation thermal conductivity, a small discrepancy of $k(p)$ curves is caused by different $k_{ss}+k_r$ components in the two types of insulations. The insulations differ from each other in the composition of the shell material, density, and thickness of the walls and slightly in diameter. Over the pressure range 10^2–10^5 Pa, where gas is the dominant medium transferring heat, the discrepancy is larger. This is caused by the different density packings of the spheres in both samples, i.e., the different porosity m. In this pressure range, the change of medium porosity strongly affects its effective thermal conductivity by changing the Knudsen number Kn.

2.2. Self-Pumping Microsphere Insulation

Simultaneous with investigating the heat transfer in microsphere insulation, considerable effort has been made to improve the thermal parameters of the insulation.

For this purpose, we have prepared the self-pumping sample, which was expected to exhibit stable thermal parameters even in the case of the low-quantity incoming gas. Another objective was to decrease the thermal conductivity in this pressure range, in which the contribution of gas to the total conductivity of the medium is observable, i.e., for pressures above 10^{-1} Pa.

For the measurements, two microsphere samples were prepared: (1) an uncoated microsphere sample with a diameter (d_m) of 130 μm and a density (γ) of 398 $kg \cdot m^{-3}$ and (2) a sample prepared by mixing microspheres with diameters the same as above with a 10% volume of powdered charcoal.

The measurements of the thermal conductivity coefficient as a function of the residual gas pressure were performed in a cylindrical calorimeter. The thickness of the insulation layer of the calorimeter is 0.52 cm. The method of thermal conductivity determination was based on the measurement of the rate of liquid nitrogen evaporation from the inner cylinder of the calorimeter. The cylindrical calorimeter makes possible the minimization of boundary effects and it is comparatively easy to make [10]. The guarded flat plate apparatus [11, 12] makes possible the realization of thermal conductivity measurements in dependence of external loading of samples. For our measurements with the cylindrical calorimeter, the maximum relative error in the k value accounted by the total differential method was 7%. The error of estimation of geometrical factors of the calorimeter was 5.4%. Other errors are related to the measurement of the velocity of nitrogen vaporization, 0.15%, and the error of estimation of the temperature difference in the sample, 1%. In Ref. 13, for the spherical

calorimeter, the authors estimated the total error of measurements to be about 3%.

The results of measurements of the thermal conductivity coefficient as a function of the residual gas pressure for a classical microsphere insulation (curve 1) and for the self-pumping microsphere insulation (curve 2) are presented in Fig. 2. One may observe a reduction of the thermal conductivity for the sample with self-pumping insulation both in the pressure range 10^{-1}–10^{2} Pa and below 10^{-1} Pa. In the latter range, the gas contribution to the total thermal conductivity of such a medium is small. A small reduction of the thermal conductivity in the pressure range below 10^{-1} Pa may be due to cooperative actions of two effects: (1) the effect caused by increasing resistance of the contact between microsphere surfaces adjoining each other as a result of the introduction of small particles of charcoal between these surfaces (the dimensions of charcoal particles are several times smaller than those of the microsphere) and (2) the effect caused by change in the extinction coefficient. The lower thermal conduc-

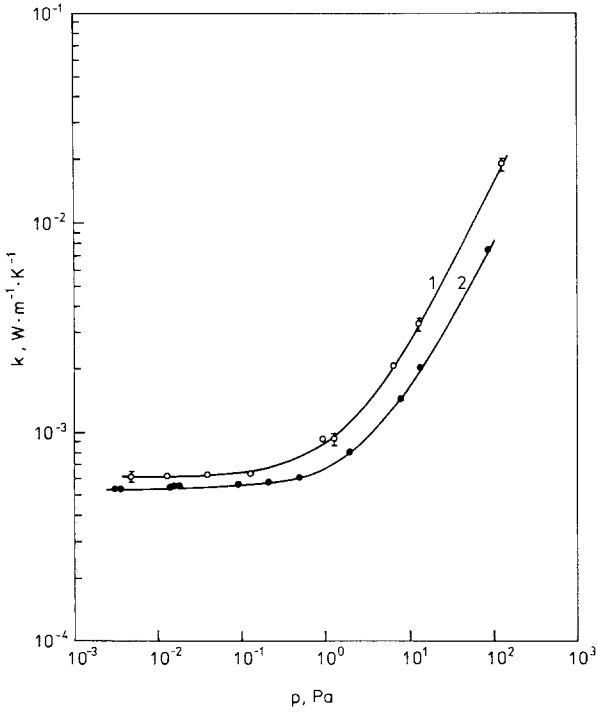

Fig. 2. Apparent thermal conductivity $k_{77\text{–}293\,K}$ vs residual gas pressure (air) for classical (Curve 1) and self-pumping (Curve 2) microsphere insulation.

tivity over the pressure range from 1 to 10^2 Pa, reaching values even lower than about 50% compared with the conductivity of classical microsphere insulation, may be due to the following two reasons:

(1) the decreasing pressure inside the layer of self-pumping insulation induced by gas absorption from the interstitial volume in the charcoal particles and

(2) a change in the mean free path of the gas particles and of the local distance between surfaces δ_a (between which a heat exchange takes place) as a result of the introduction of charcoal particles to the interstitial volume. The change in value of these two parameters results in a variation of the Knudsen number $\bar{L}/\delta_a$.

Another value of an extinction coefficient for self-pumping insulation has a relatively small influence on the change of the total thermal conductivity in this pressure range.

While conducting the measurement of $k(p)$ another experiment was performed; the volume and pressure of air which was introduced into the calorimeter were controlled. The results obtained are presented in Table I. For traditional microsphere insulation the introduction of air with a volume of $v = 0.085\ \text{cm}^3$ under a pressure of 101, 325 Pa (which

Table I. Comparison of the Characteristic Parameters for the Classical and Self-Pumping Microsphere Insulations

Microsphere insulation			Self-pumping microsphere insulation		
Volume of air introduced into the calorimeter under a pressure of 101,325 Pa, v (cm^3)	Pressure inside the calorimeter, p_0 (Pa)	Apparent thermal conductivity, $k_{77\ 292\,K} \times 10^4$ ($\text{W} \cdot \text{m}^{-1} \cdot \text{K}^{-1}$)	Volume of air introduced into the calorimeter under a pressure of 101,325 Pa, v (cm^3)	Pressure inside the calorimeter p_0 (Pa)	Apparent thermal conductivity, $k_{77\ 292\,K} \times 10^4$ ($\text{W} \cdot \text{m}^{-1} \cdot \text{K}^{-1}$)
0	5.3×10^{-3}	6.1	0	3.7×10^{-3}	5.3
0.085	9.5×10^{-1}	9.2	0.07	1.6×10^{-2}	5.5
0.190	6.0	19.6	0.18	1.5×10^{-2}	5.4
			0.36	9.3×10^{-2}	5.6
			0.45	2.1×10^{-1}	5.7
			0.91	5.1×10^{-1}	6.2
			3.37	2.0	8.0
			10.53	8.3	14.2
			6.53	14.7	20.0
			21.06	106.7	72.5

corresponds to a volume of 64.6 cm^3 under a pressure of 133.3 Pa) caused the decreasing vacuum from 5.3×10^{-3} to 9.5×10^{-1} Pa. At the same time an increase in the thermal conductivity of the insulation from 6.1 to 9.2×10^{-4} $W \cdot m^{-1} \cdot K^{-1}$ was observed. Introducing air with a volume $v = 0.19$ cm^3 depressed the vacuum to 6 Pa and the thermal conductivity increased to 19.6×10^{-4} $W \cdot m^{-1} \cdot K^{-1}$. However, for the self-pumping microsphere insulation the introduction of a similar quantity of air to the insulating volume decreased the vacuum only to 1.5×10^{-2} Pa, keeping k constant.

In order to increase the thermal conductivity coefficient to 20×10^{-4} $W \cdot m^{-1} \cdot K^{-1}$ it was necessary to introduce as much as 22.4 cm^3 of air under atmospheric pressure into the calorimeter.

2.3. Temperature and Pressure Gradients Inside the Layer of Microsphere Insulation

In order to understand more completely the heat transfer mechanisms, measurements of the temperature distribution inside the microsphere layer were conducted. The measurements were performed in a cylindrical calorimeter (Fig. 3) having an insulation layer of 40 mm and a height of 300 mm. Inside the microsphere layer, four tubes were immersed (tube diameter, 5 mm; distance from calorimeter axis, $r_1 = 43.38$ mm, $r_2 = 52.96$ mm, $r_3 = 62.96$ mm, and $r_4 = 73.38$ mm). These tubes were connected to independent vacuum gauges. In each set, the resistance pressure sensor used was of the platinum GN-42 type, and the ionization gauge of the SJ-2 type. The same set of gauges was used for measurements of the p_0 pressure above the insulation layer. Each tube, at its lower end, was equipped with a filter made of phosphorobronze, with dimensions of the holes smaller than the sphere diameter. This type of filter prevents microspheres from penetrating inside the tube. For measurements of the temperature distribution inside the microsphere bed, a constantan–manganin thermocouple was used. The thermocouple wire had a diameter of 50 μm and was glued to each tube with BF-2.

Figure 4 presents the temperature distribution inside the microsphere bed with granule dimensions in the range 40 to 400 μm. Here, the independent parameter is the residual gas pressure p_0 above the insulation bed. Temperatures at the points where tubes and thermocouples are located inside the microsphere layer, at a distance of $(r_i - 40)$ mm, where $i = 1, 2, 3, 4$ from the cold wall of the calorimeter, were measured under steady-state heat flow conditions.

In the case of a high vacuum at a distance as small as 5 mm from the calorimeter wall cooled down to 77 K, the temperature reaches a high

value of 200 K, however, for $p_0 = 133.3$ Pa the temperature at the same point is only 120 K. This proves the existence of a large temperature gradient near the cold wall of the calorimeter, as may be seen in Fig. 5. For pressure $p_0 = 1.87 \times 10^{-3}$ Pa, the maximum value of dT/dr is higher than $60\ \mathrm{K \cdot mm^{-1}}$ near the cold wall of the calorimeter. For a residual gas pressure of the order of 133.3 Pa this value is reduced to about $10\ \mathrm{K \cdot mm^{-1}}$ (Fig. 6).

Figure 7 shows the pressure distribution inside the microsphere bed over the pressure range from 1×10^{-1} to 10 Pa. For determination of the gas pressure inside the insulation bed the following formula was used:

$$p = \frac{p_g (T_i)^{1/2}}{T_g^{1/2}} \tag{5}$$

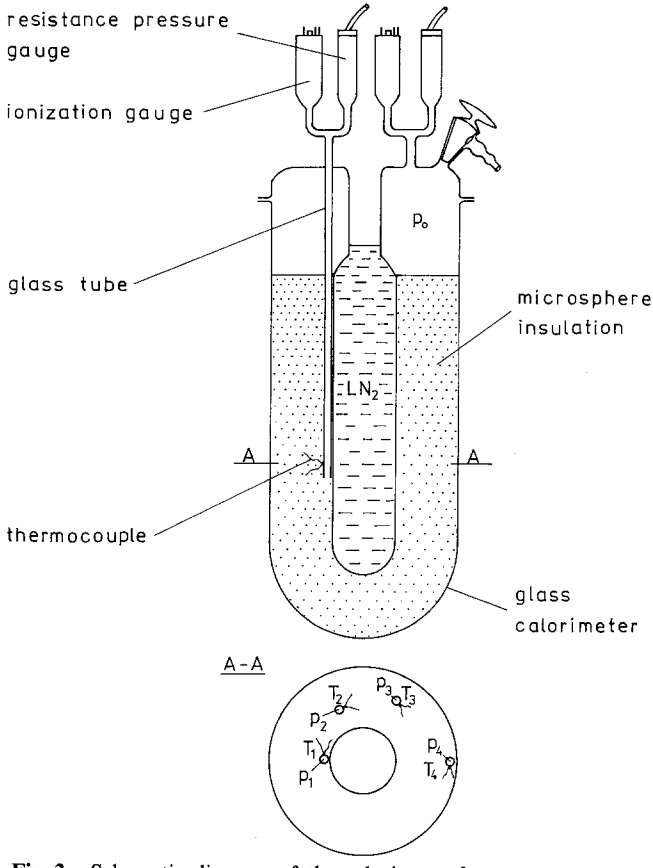

Fig. 3. Schematic diagram of the calorimeter for measurements of distributions of temperature and pressure inside the microsphere insulation bed.

Prior to the measurements, the insulation sample was outgassed to the pressure of $p_0 = 8 \times 10^{-1}$ Pa and subsequently the calorimeter was filled with liquid nitrogen. During the initial stage of the insulation cooling, a decrease in the pressure inside the layer and p_0 was observed. This is related to condensation of water vapor, carbon dioxide, and other gases on the cold calorimeter wall and on microsphere walls in the vicinity of the cold calorimeter wall (the curve for $\mathcal{T} = 5$ min). For time $\mathcal{T} = 30$ min, one may observe only a decrease in the pressure inside the insulation layer and an increase in the p_0. Next, the pressure inside the layer and p_0 increase with time as the result of gas desorption from the shell material and diffusion from the microsphere interior.

The plot of $p(r)$ curves for times $\mathcal{T} = 5$ and 30 min is sharper in this half of the layer which is nearer to the cold wall of the calorimeter

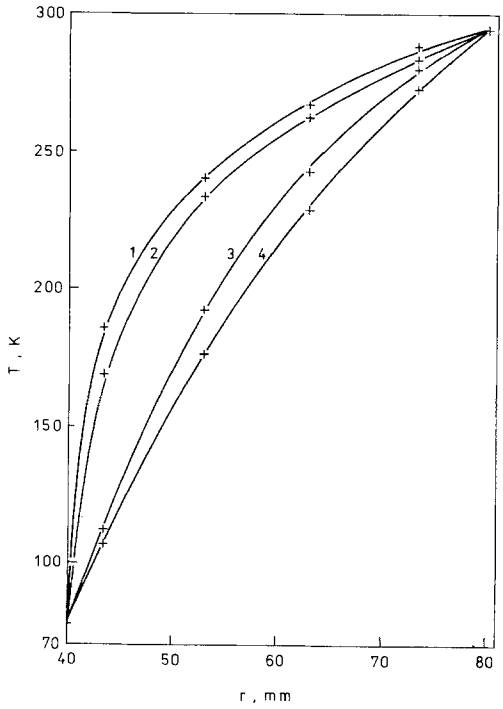

Fig. 4. The temperature distribution inside the microsphere insulation bed (for $r = 40$ mm, $T = 77$ K; for $r = 80$ mm, $T = 297$ K). Curve 1, $p_0 = 1.9 \times 10^{-3}$ Pa; Curve 2, $p_0 = 3.5 \times 10^{-1}$ Pa; Curve 3, $p_0 = 9.5$ Pa; Curve 4, $p_0 = 133.3$ Pa.

(40 mm $< r <$ 60 mm). It means that a large pressure gradient dp/dr exists in this range. The curves $p(r)$ for $\mathcal{T} = 125$, 405, 1225, and 2825 min represent polynomials of the second order. From differentiation of the $p(r)$ dependences, one may conclude the existence of pressure gradients perpendicular to the heat flux direction in the case of curves 2, 3, and 4 (Fig. 8).

The results obtained prove the existence of a large pressure gradient in the vicinity of the calorimeter cold wall at the initial stage of sample cooling (curves 1 and 2) in Fig. 8. The dp/dr versus r plots obtained from the rest of the $p(r)$ curves have a linear character with a small slope (curves 3, 4, 5, and 6) in Fig. 8. After the establishment of the steady-state heat flow in the insulation, pressure p_0 reaches values close to those of the average pressure inside the layer without removing the gas outside the calorimeter. However, while evacuating the insulation space to a pressure of the order of 10^{-3} Pa, p_0 reaches a value about two times lower than the average pressure inside the insulation layer.

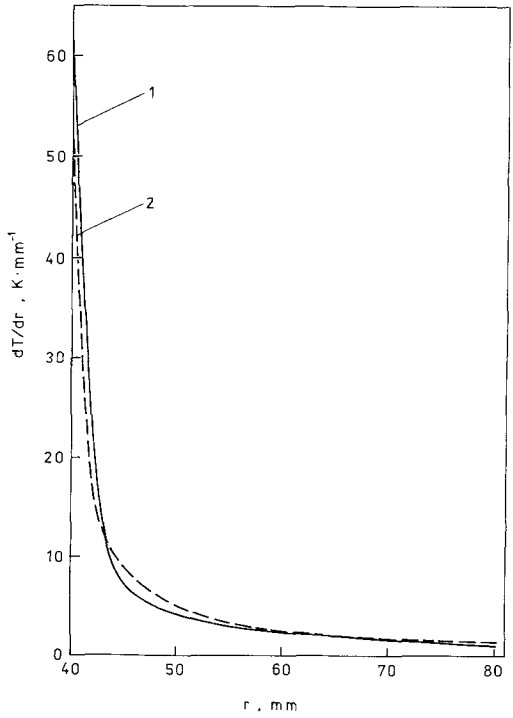

Fig. 5. Temperature gradient vs radial coordinate in the microsphere insulation. Curve 1 (——), $p_0 = 1.9 \times 10^{-3}$ Pa; Curve 2 (- - - - - - -), $p_0 = 3.5 + \times 10^{-1}$ Pa.

Measurements of the pressure distribution made with ionization gauges, for $p < 10^{-1}$ Pa, do not give reliable results because of decomposition of water particles in the ionization gauge. The existence of uncondensating hydrogen at these temperatures reduces the pressure gradient to values nondetectable by ionization gauges. Another reason which makes pressure distribution measurements unreliable is the gas "pumping" by the ionization gauges. So the problem of the measurements of pressure distribution inside the layer of microsphere insulation in the pressure range below 10^{-1} Pa still remains unresolved.

3. CONCLUSIONS

It is concluded that in the range of higher residual gas pressure, i.e., from 10^2 Pa to ambient pressure, the thermal conductivity of the insulation is influenced mainly by the packing density of the microspheres (Fig. 1).

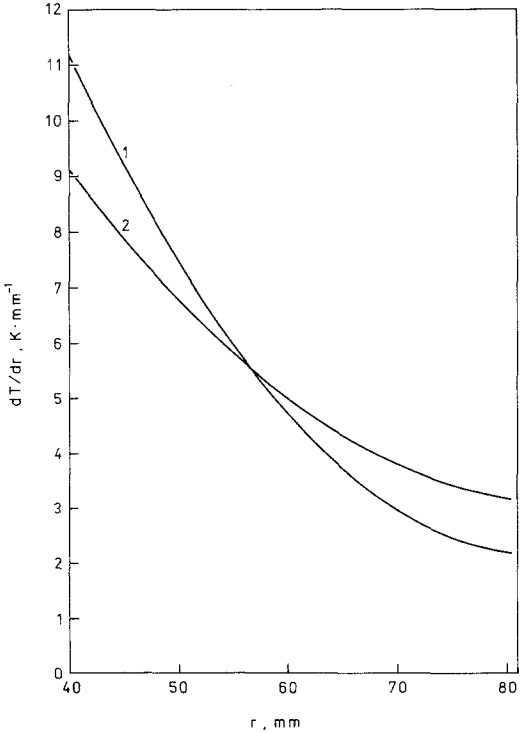

Fig. 6. Temperature gradient vs radial coordinate in the microsphere insulation. Curve 1, $p_0 = 9.5$ Pa; Curve 2, $p_0 = 133.3$ Pa.

The change in the medium porosity strongly changes the Knudsen number. This is expressed satisfactorily by Eq. (2) since, for the two different types of microspheres investigated in different laboratories, a satisfactory agreement was obtained between the results calculated by this equation and the experimental data.

For self-pumping insulation a decrease in the thermal conductivity was obtained. Despite the income of considerable amounts of gas to the insulation volume, a stability in the thermal parameters of the insulation has been observed.

The results of measurements of the temperature distribution inside the layer of microsphere insulation show the existence of large temperature gradients near the cold wall of the calorimeter in the case of a high

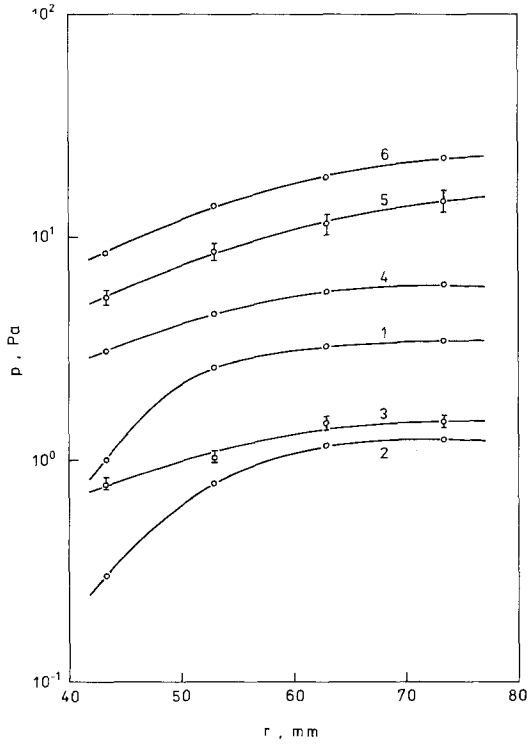

Fig. 7. Gas pressure distribution inside the microsphere insulation bed. Curve 1, $p_0 = 1.33 \times 10^{-2}$ Pa, $\mathscr{T} = 5$ min; 2, $p_0 = 2.93 \times 10^{-1}$ Pa, $\mathscr{T} = 30$ min; 3, $p_0 = 7.73 \times 10^{-1}$ Pa, $\mathscr{T} = 125$ min; 4, $p_0 = 5.6$ Pa, $\mathscr{T} = 405$ min; 5, $p_0 = 12.9$ Pa, $\mathscr{T} = 1225$ min; 6, $p_0 = 21.3$ Pa, $\mathscr{T} = 2825$ min.

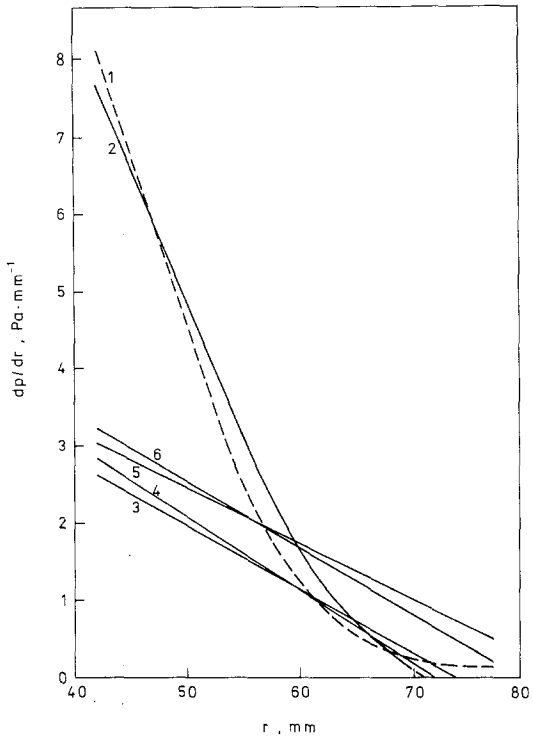

Fig. 8. Pressure gradient vs radial coordinate in the microsphere insulation. Curve 1, $p_0 = 1.33 \times 10^{-2}$ Pa, $\mathscr{T} = 5$ min; 2, $p_0 = 2.93 \times 10^{-1}$ Pa, $\mathscr{T} = 30$ min; 3, $p_0 = 7.73 \times 10^{-1}$ Pa, $\mathscr{T} = 125$ min; 4, $p_0 = 5.6$ Pa, $\mathscr{T} = 405$ min; 5, $p_0 = 12.9$ Pa, $\mathscr{T} = 1225$ min; 6, $p_0 = 21.3$ Pa, $\mathscr{T} = 2825$ min.

vacuum, which means that this type of insulation is very effective. However, pressure distribution measurements demonstrated the existence of small linear pressure gradients along the direction of the heat flux.

ACKNOWLEDGMENTS

The authors are indebted to Dr. K. Balcerek for the initiation of the investigations of self-pumping microsphere insulation and Mr. T. Tyc and Dr. P. Markowski for helping in the preparation of the paper.

NOMENCLATURE

d_m Mean value of the microsphere diameter
k Apparent thermal conductivity coefficient
$\bar{k}$ Average thermal conductivity coefficient
k_c Component of the heat transfer by conduction
k_g Modified gas thermal conductivity under atmospheric pressure
k_r Component of the heat transfer by radiation
k_s Thermal conductivity of the sphere material
k_{gc} Component of the heat conduction by gas
k_{go} Gas thermal conductivity under atmospheric pressure
k_{gr} Sphere effective conductivity
k_{ss} Component of the heat conduction by the solid state
K $1-(k_g/k_{gr})$
Kn Knudsen number
$\bar{L}$ Mean free path of gas molecules
m $1-\delta_s$; porosity
m' Empty volume of a single sphere
p Residual gas pressure
$\bar{p}$ Average pressure
p_g Pressure measured by gauge
p_0 Residual gas pressure above the insulation bed
r Radial coordinate
T Temperature
T_C Temperature of the cold calorimeter wall
T_g Temperature of the pressure gauge
T_H Temperature of the hot calorimeter wall
T_i Gas temperature inside the bed
T_y Constant dependent on the sort of gas
v Volume
α Accommodation coefficient
γ Density
δ_a Local distance between surfaces
δ_s Solid fraction
κ Constant dependent on the sort of gas
$\mathscr{T}$ Time measured from the initiation of insulation cooling

REFERENCES

1. R. G. Scurlock and B. Saul, *Cryogenics* **16**:303 (1976).
2. R. Wawryk and K. Balcerek, Thermal conductivity of hollow glass microsphere insulation in the temperature range 80–300 K. Paper presented at the 7th European Thermophysical Properties Conference, Antwerpen (1980).

3. G. R. Cunnington and C. L. Tien, *Adv. Cryogen. Eng.* **22**:263 (1977).
4. R. Wawryk and J. Rafałowicz, *Cryogenics* **25**:33 (1985).
5. M. G. Kaganer, *Thermal Insulation in Low Temperature Technics* (Moscow, 1966) (in Russian).
6. M. G. Kaganer, *Heat and Mass Transfer in Low-Temperature Designs* (Energia Press, Moscow, 1979) (in Russian).
7. W. A. Osipova, *Experimental Investigations of Heat Exchange Processes* (Energia Press, Moscow, 1964) (in Russian.
8. R. H. Kropschot, B. L. Knight, and K. D. Timmerhaus, *Adv. Cryogen. Eng.* **14**:224 (1969).
9. G. R. Cunnington and C. L. Tien, in *Thermal Conductivity 15*, V. V. Mirkovich, ed. (Plenum, New York, 1978), p. 325.
10. R. H. Kropschot and R. W. Burgess, *Adv. Cryogen. Eng.* **8**:425 (1963).
11. D. Büttner, J. Fricke, R. Krapf, and H. Reiss, *High Temp. High Press.* **15**:233 (1983).
12. H. Reiss, F. Schmaderer, G. Wahl, B. Ziegenbein, and R. Caps, *Int. J. Thermophys.* **8**:263 (1987).
13. A. L. Nayak and C. L. Tien, *Adv. Cryogen. Eng.* **22**:251 (1977).